# Structure and Thermal Vibrations of Spermine Phosphate Hexahydrate from Neutron Diffraction Data at 125 K

A. E. Cohen,[a] B. M. Craven[a]* and W. T. Klooster[b]

[a]*Department of Crystallography, University of Pittsburgh, Pittsburgh, PA 15260, USA, and* [b]*Chemistry Department, Brookhaven National Laboratory, Upton, NY 11973, USA. E-mail: craven@vms.cis.pitt.edu*

## Abstract

Spermine phosphate hexahydrate crystallizes in space group $P2_1/a$ with unit-cell dimensions $a = 7.931$ (1), $b = 23.158$ (5), $c = 6.856$ (2) Å, and $\beta = 113.44$ (2)° at 125 K with unit-cell contents $[(C_{10}H_{30}N_4)_2^{4+}(HPO_4)_4^{2-}.12H_2O]$. The packing of spermines and monohydrogen phosphates in this crystal structure has features which may be relevant to the binding of spermine to DNA. Another important structural feature is the presence of channels containing water that is hydrogen bonded as in ice-Ih with disordered protons. The channels occur between sheets of spermine long chains and are also bordered by hydrogen-bonded monohydrogen phosphate chains. The hydrogen-bonding scheme of these water chains proposed on the basis of an earlier X-ray study is now confirmed. Nuclear positions, anisotropic mean-square (m.s.) displacements, an overall scale factor and two extinction parameters ($\rho$ and $g$) were refined using full-matrix least-squares giving values of $R(F_o^2) = 0.09$, $Rw(F_o^2) = 0.11$ and $S = 1.02$. Thermal vibrational analysis revealed that the backbone of the spermine cation can be described as a single rigid segment with a substantial libration of $27 \deg^2$ around the spermine molecular long axis.

## 1. Introduction

Spermine ($C_{10}H_{26}N_4$) is a very water-soluble, strongly basic, aliphatic polyamine widely found in nature. Crystals of spermine phosphate hexahydrate were first observed and described by van Leeuwenhoek (1678). Spermine has a strong affinity for nucleic acids and affects the rate and extent of nucleic acid biosynthesis (for reviews, see Tabor & Tabor, 1976; Morris & Marton, 1981). The crystal structure of spermine phosphate hexahydrate† was first determined by Iitaka & Huse (1965) from X-ray Weissenberg photographic data, but the hydrogen positions were not located. This structure is well suited for a more detailed crystallographic study.

† $[(C_{10}H_{30}N_4)_2^{4+}(HPO_4)_4^{2-}.12H_2O]$, sperminium monohydrogen phosphate hexahydrate, is referred to as spermine phosphate hexahydrate in accordance with previously published works and in this text will be subsequently designated as SPH.

It has a centrosymmetric space group, so that there are no ambiguities in phasing the structure factors, and the spermine tetracation lies on a crystallographic inversion center so that the asymmetric unit consists of only half a molecule. Finally, the crystal structure includes water molecules, which display an interesting ice-like configuration. This neutron diffraction study is aimed at providing accurate positional and thermal-vibrational parameters of the atomic nuclei for use in the study of the charge density distribution in the crystal from X-ray data collected at the same low temperature.

## 2. Experimental

Crystals of SPH were formed by very slow cooling of a solution of spermine phosphate (Sigma Chemical Company) in the presence of phosphoric acid. Differential scanning calorimetry on large single crystals, using a Mettler TA4000 system, showed no crystal phase transitions as the temperature was lowered from room temperature down to 115 K. The crystal used for neutron diffraction data collection was elongated along the $c$ axis, with well developed (010) faces. The crystal dimensions were approximately $3.4 \times 0.75 \times 1.5$ mm and the crystal mass was 4 mg. The crystal was glued to a hollow aluminum pin and placed into an aluminum can, which was then sealed and filled with helium. The crystal was then cooled to 125 K using a closed-cycle refrigerator.† Neutron data were collected using the four-circle diffractometer at the H6S station of the High Flux Beam Reactor at Brookhaven National Laboratory. The 220 reflection from a germanium crystal was used to obtain a monochromatic neutron beam with wavelength 1.16395 (10) Å. The unit-cell dimensions, $a = 7.931$ (1), $b = 23.158$ (5), $c = 6.856$ (2) Å, and $\beta = 113.44$ (2)° at 125.0 (5) K with two formula units in the unit cell, were determined through a least-squares fit of setting angles for 32 reflections in the range $50 < 2\theta < 61°$. The integrated intensity data were obtained by means of $\omega/2\theta$ step scans for the quadrant of reciprocal space having indices ranging from $-10$ to 10 in $h$, 0 to 33 in $k$ and 0 to 9 in $l$. The data collection was divided into two

† DISPLEX model CS-202, APD Cryogenics, Inc.

shells with $\sin \theta/\lambda$ limiting values of 0.43 and 0.68 Å$^{-1}$. Scan widths were constant in the first shell ($\Delta 2\theta$ = 2.4°), but variable for the second shell [$\Delta 2\theta$ = 1.097° + 5.935$\tan(\theta)$]. Two standard reference reflections (412 and $\overline{6}$92) measured at intervals of 50 reflections showed no significant variation of intensity with time. A total of 3378 reflections were measured. Data processing was carried out by a series of computer programs developed by Blessing (1989), which were all modified for use with neutron diffraction data. Integrated intensities and variances were derived from the scan profiles. Each scan profile was examined (Spackman, 1987) and, if necessary, the scan limits were shifted to exclude contributions to the background by neighboring reflections and aluminum powder lines. Peak overlap was very severe for 135 reflections, which were therefore omitted. An analytical correction for neutron absorption with $\mu$ = 0.345 mm$^{-1}$ was made (Templeton & Templeton, 1973). Transmission factors ranged between 0.60 and 0.76, with an average factor of 0.72. Symmetry-related reflections were found to be in good agreement, $R(F_o^2)_{int}$ = 0.015 [$R(F^2)_{int}$ = $\Sigma_i |{<}F_o^2{>} - F_o^2|/\Sigma{<}F_o^2{>}$], and were averaged to give 2873 independent observations. Of these reflections, 2446 had intensities greater than $2\sigma$ and 2 reflections were in the range between $-2\sigma$ and $-5\sigma$.

## 2.1. Structure refinement

Using initial non-H-atom positions from the X-ray study of Iitaka & Huse (1965) the crystal structure was first refined by differential Fourier synthesis (McMullan, 1976). A difference-Fourier map revealed the nondisordered hydrogen positions. The disordered hydrogen positions were located from examination of a Fourier map (Shiono, 1972). All reflections were subsequently included in a full-matrix least-squares refinement (Craven & Weber, 1987), in which extinction is treated according to Sabine (1992$a$). The residual $\Sigma w\Delta^2$ was minimized with $w = \sigma^{-2}(F_o^2)$ and $\Delta = F_o^2 - F_c^2$. A total of 354 variables were refined, including nuclear positions, anisotropic m.s. displacements, an overall scale factor and two extinction parameters ($\rho$ and $g$). The 003 reflection was most affected by extinction ($y$ = 0.58, where $y = I_o^{ext}/I_k$). Coherent scattering lengths were assumed to be 6.648, 9.360, 5.803 and $-3.741$ fm for carbon, nitrogen, oxygen and hydrogen, respectively (Koester, 1977). The refinement was completed with $R(F_o^2)$ = 0.09, $wR(F_o^2)$ = 0.11 and $S$ = 1.02 with 2519 degrees of freedom.† Final values of the nuclear parameters are listed in Table 1. The extinction parameters, obtained for a model with crystal mosaic blocks scattering without correlations in phases (Sabine, 1992$b$), give a Gaussian distribution of mosaic blocks with a standard deviation of $\eta$ = 0.58 (3)″, where $\eta = 1/(2\pi^{1/2}g)$ and a block size of 361 (10) μm.

† $R(F^2) = (\Sigma|\Delta|)/\Sigma F_o^2$, $wR(F^2) = [(\Sigma w\Delta^2)/(\Sigma wF_o^2)^2]^{1/2}$, $S = [(\Sigma w\Delta^2)/(m - n)]^{1/2}$, where $\Delta = |F_o|^2 - |F_c|^2$.

Table 1. *Fractional atomic coordinates for SPH*

$$U_{eq} = (1/3)\Sigma_i\Sigma_j U^{ij}a_i^* a_j^* \mathbf{a}_i.\mathbf{a}_j.$$

| | $x$ | $y$ | $z$ |
|---|---|---|---|
| N1 | 0.7107 (1) | 0.09375 (6) | −0.0027 (3) |
| N2 | 0.1646 (2) | 0.21083 (6) | −0.0627 (2) |
| C1 | 0.9656 (2) | 0.03124 (8) | −0.0094 (3) |
| C2 | 0.7785 (3) | 0.03342 (8) | 0.0018 (3) |
| C3 | 0.5206 (2) | 0.09474 (8) | −0.0117 (3) |
| C4 | 0.4468 (3) | 0.15576 (8) | −0.0264 (3) |
| C5 | 0.2535 (2) | 0.15316 (8) | −0.0302 (3) |
| W1 | 0.1176 (4) | 0.0467 (1) | 0.5460 (4) |
| W2 | 0.4170 (3) | 0.0529 (1) | 0.4380 (4) |
| W3 | 0.6652 (3) | 0.1465 (1) | 0.5978 (4) |
| P | −0.0047 (3) | 0.19654 (9) | 0.3684 (4) |
| O1 | −0.0735 (3) | 0.21066 (9) | 0.1328 (3) |
| O2 | −0.0233 (3) | 0.24703 (9) | 0.5021 (4) |
| O3 | −0.0980 (3) | 0.14162 (9) | 0.4011 (3) |
| O4 | 0.2072 (3) | 0.18018 (9) | 0.4534 (4) |
| H1N1 | 0.7135 (5) | 0.1164 (2) | −0.1343 (7) |
| H2N1 | 0.7945 (5) | 0.1155 (2) | 0.1370 (7) |
| H1C1 | 1.0635 (6) | 0.0575 (2) | 0.1171 (7) |
| H2C1 | 0.9571 (6) | 0.0495 (2) | −0.1614 (7) |
| H1C2 | 0.7834 (6) | 0.0134 (2) | 0.1490 (7) |
| H2C2 | 0.6762 (5) | 0.0106 (2) | −0.1341 (7) |
| H1C3 | 0.5226 (6) | 0.0731 (2) | 0.1309 (8) |
| H2C3 | 0.4335 (6) | 0.0693 (2) | −0.1505 (7) |
| H1C4 | 0.4419 (6) | 0.1769 (2) | −0.1720 (7) |
| H2C4 | 0.5367 (6) | 0.1812 (2) | 0.1124 (8) |
| H1C5 | 0.2561 (6) | 0.1363 (2) | 0.1211 (7) |
| H2C5 | 0.1665 (6) | 0.1246 (2) | −0.1583 (8) |
| H1N2 | 0.0638 (5) | 0.2111 (2) | 0.0009 (7) |
| H2N2 | 0.1025 (6) | 0.2222 (2) | −0.2235 (6) |
| H3N2 | 0.2651 (2) | 0.2427 (4) | 0.0192 (6) |
| H1W1† | 0.2170 (20) | 0.0500 (4) | 0.5026 (16) |
| H2W1 | 0.0431 (6) | 0.0822 (2) | 0.4979 (7) |
| H3W1† | 0.0361 (13) | 0.0161 (4) | 0.5162 (15) |
| H1W2 | 0.4932 (7) | 0.0870 (2) | 0.4877 (8) |
| H2W2 | 0.3110 (4) | 0.0553 (5) | 0.4731 (17) |
| H3W2† | 0.4847 (14) | 0.0184 (5) | 0.4805 (17) |
| H1W3† | 0.7557 (6) | 0.1460 (2) | 0.5333 (7) |
| H2W3 | 0.6056 (6) | 0.1844 (2) | 0.5632 (7) |
| HO4 | 0.2956 (5) | 0.2119 (2) | 0.4598 (6) |

† Disordered atoms with occupancy 0.5.

## 2.2. Thermal vibrational analysis

In Figs. 1 and 2 it can be seen that the 50% probability ellipsoids enclosing the hydrogen nuclei of the spermine tetracation and monohydrogen phosphate are consistently larger than those for the C, N, O and P nuclei. The considerably greater size of the H-ellipsoids suggests that for the hydrogen nuclei, intramolecular nonrigid C—H, N—H and O—H thermal vibrations are appreciable. The difference in m.s. amplitudes of nuclear displacement along the interatomic vector for nuclei $A$ and $B$ was determined from $U_{obs}^{ij}$, $\Delta(A,B) = {<} u_B^2 {>}{<} u_A^2 {>}$. A significant nonzero value for $\Delta(A,B)$ indicates that nuclei $A$ and $B$ are vibrating nonrigidly (Hirshfeld, 1976). The Hirshfeld test (Hirshfeld, 1976) indicates nonrigidity for nuclear vibrations in monohydrogen phosphate along interatom vectors involving the H atom. Along the HO4—O4 bond, $\Delta$ = 0.0065 (26) Å$^2$ with a significance level of 2.5$\sigma$. For the heavier atoms, values of $\Delta$ are small. The largest of these, $\Delta$ = 0.0025 (14) Å$^2$, is along the P—O3 bond direction. Also, for the non-H backbone of the spermine cation values of $\Delta(A,B)$

are very small and insignificant; for example, $\Delta$ = 0.0002 (13) $\text{Å}^2$ for N2$\cdots$C5' and the largest difference is $\Delta$ = 0.0027 (16) $\text{Å}^2$ for C4$\cdots$C5. In contrast, nonrigidity is strongly indicated for most covalent bonds involving H atoms (Table 2). For instance, along the C4—H2C4 bond, $\Delta$ = 0.0077 (22) $\text{Å}^2$ and along the N1—H2N1 bond, $\Delta$ = 0.0067 (19) $\text{Å}^2$.

Analysis of nuclear anisotropic m.s. displacements for the hydrogen nuclei of the spermine cation (Table 1) began by using the simple rigid-body model (Schomaker & Trueblood, 1968) for the backbone (C and N) nuclear vibrations. Because the cation has a crystallographic center of symmetry, only the rigid body $\mathbf{T}$ and $\mathbf{L}$ tensors need be considered. The residual, $\Sigma w(U^{ij}_{\text{obs}} - U^{ij}_{\text{calc}})^2$ with $w = 1/\sigma^2(U_{\text{eq}})$, was minimized by least-squares (He & Craven, 1993), giving an agreement with $wR$ = 0.088 and $S$ = 1.23 ($wR$ = $[(\Sigma w\Delta^2)/(\Sigma wU^{ij}_{\text{obs}})^2)]^{1/2}$, where $\Delta$ = $U^{ij}_{\text{obs}} - U^{ij}_{\text{calc}}$) and the sum includes all six $U^{ij}$ components for all atomic nuclei; $S$ = $[\Sigma w\Delta^2/(m - n)]^{1/2}$ with $(m - n)$ = 72). In the least-squares fit the $T_{11}$ (translation normal to the plane of the C and N nuclei) and $L_{33}$ tensor components (libration around the molecular long axis) are highly correlated (94%),
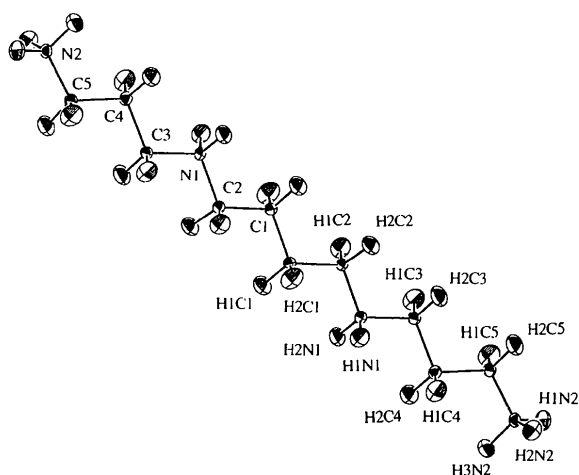


Fig. 1. Thermal ellipsoid plot for the spermine tetracation at 50% probability for enclosing the atomic nuclei (Johnson, 1976).
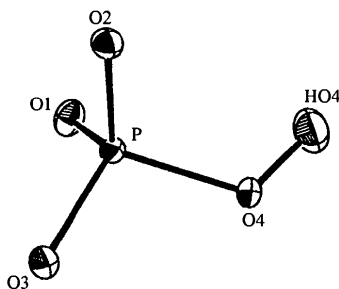


Fig. 2. Thermal ellipsoid plot for the monohydrogen phosphate ion at 50% probability for enclosing the atomic nuclei (Johnson, 1976).

because the atomic nuclei of the molecular backbone lie nearly on one of two parallel straight lines (Johnson, 1970). In order to overcome this problem anisotropic m.s. displacement parameters of the methylene H nuclei were added to the rigid-body calculation. Before a rigid-body model can be fitted to the observed anisotropic thermal vibrations of hydrogen atomic nuclei, it is necessary to correct for the internal molecular motion of the hydrogen nuclei (Johnson, 1970). Values of the internal m.s. displacements of methylene H nuclei, $U^{ij}_{\text{int}}$, were taken from a previous neutron diffraction study of piperazinium hexanoate (Luo, Ruble, Craven & McMullan, 1996). The average principal values of the internal m.s. displacements of methylene H nuclei used were $U_1$ = $5 \times 10^{-4}$, $U_2$ = $174 \times 10^{-4}$ and $U_3$ = $174 \times 10^{-4}\,\text{Å}^2$, where $U_1$ corresponds to bond stretching along the C—H bond, $U_2$ is a displacement in the H—C—H plane and $U_3$ is a displacement normal to the H—C—H plane. The residuals, assumed to represent the external component of the anisotropic m.s. displacements for the methylene H nuclei, $U^{ij}_{\text{ext}}$, and the observed m.s. displacements, $U^{ij}_{\text{obs}}$, for the framework nuclei (C and N) were all included in a subsequent least-squares fit to the rigid-body model. A good fit was obtained with $wR$ = 0.114 and $S$ = 1.162, where $(m - n)$ = 192. The correlation between $T_{11}$ and $L_{33}$ became insignificant and a substantial libration [$L_{33}$ = 27 (1) $\text{deg}^2$] around the molecular long axis was obtained. The Hirshfeld test (Hirshfeld, 1976) does not rule out the presence of internal torsional vibrations of the chain since these involve displacements close to the normal of the planar spermine backbone. Such torsional modes were found for the hydrocarbon chain in suberic acid (Gao, Weber, Craven & McMullan, 1994). Although models of this type were tested, none gave improved agreement over the simple rigid-body model for the spermine chain. The value of $L_{33}$ is certainly an overestimate because it includes the effect of nonrigid modes.

The rigid-body parameters listed in Table 2 were then used in order to calculate the rigid-body contribution to the m.s. displacements of each amine H nucleus. This value was subtracted from $U^{ij}_{\text{obs}}$ for each ammonium H nucleus to give $U^{ij}_{\text{int}}$, the intramolecular component of the m.s. displacements. These residual values were transformed to a local Cartesian axial system with $U^{11}_{\text{int}}$ along the N—H bond, $U^{22}_{\text{int}}$ in the plane of the NH$_2$ group and normal to the N—H bond, and $U^{33}_{\text{int}}$ along the normal to the plane of the NH$_2$ group. Thus, $U^{11}_{\text{int}}$ corresponds to bond stretching along the N—H bond, $U^{22}_{\text{int}}$ is a displacement in the H—N—H plane and $U^{33}_{\text{int}}$ is a displacement normal to the H—N—H plane.† Table 2 shows these values of $U^{ij}_{\text{int}}$ with respect to the local Cartesian axial system described above, as well as the principal values of these tensors in the local axial system.

† For NH$_3$, $U^{11}_{\text{int}}$ corresponds to bond stretching along the N—H bond, $U^{22}_{\text{int}}$ is an umbrella-type vibration in the C—N—H plane and $U^{33}_{\text{int}}$ is an internal torsional libration about the C—N bond.

## Table 2. *Analysis of the nuclear m.s. displacement parameters*

### (a) Molecular framework vibrations

Both the spermine and the monohydrogen phosphate ions are each treated as having one rigid segment. The rigid-body $T$, $L$ and $S$ tensor components (Schomaker & Trueblood, 1968) are with respect to the principal axes of the moments of inertia with the origin at the center of mass. The axes $I_1$, $I_2$ and $I_3$ are in the order of decreasing moment of inertia; such that for the spermine cation, $I_1$ is normal to the best plane of the framework (C and N) nuclei and $I_3$ is along the molecular long axis. The first column is for the rigid-body calculation for the spermine cation which includes $U^{ij}_{ext}$, calculated external m.s. displacement parameters of the methylene H atoms, as well as $U^{ij}_{obs}$ of the molecular framework (C and N) atoms. The second column is for the monohydrogen phosphate anion with the H atom omitted from the rigid-body calculation.

|  | Spermine cation | Monohydrogen phosphate anion |
|---|---|---|
| **Translational tensor, T ($\text{Å}^2 \times 10^4$)** | | |
| $T_{11}$ | 141 (3) | 95 (7) |
| $T_{22}$ | 107 (3) | 115 (7) |
| $T_{33}$ | 100 (2) | 87 (7) |
| $T_{12}$ | $-9$ (3) | $-9$ (6) |
| $T_{13}$ | $-3$ (2) | $-13$ (6) |
| $T_{23}$ | 15 (2) | 9 (5) |
| **Principal values** | | |
|  | 145 | 96 |
|  | 115 | 123 |
|  | 88 | 77 |
| **Librational tensor, L (deg$^2$)** | | |
| $L_{11}$ | 0 (1) | 8 (3) |
| $L_{22}$ | 0 (1) | 7 (3) |
| $L_{33}$ | 27 (1) | 6 (3) |
| $L_{12}$ | 0 (1) | 2 (2) |
| $L_{13}$ | 0 (1) | 2 (2) |
| $L_{23}$ | 0 (1) | 1 (2) |
| **Principal values** | | |
|  | 0 | 11 |
|  | 0 | 6 |
|  | 27.2 | 5 |
| **Cross Tensor, S (Ådeg $\times 10^2$)†** | | |
| $S_{11}$ | 0 | 5 (5) |
| $S_{12}$ | 0 | $-2$ (2) |
| $S_{13}$ | 0 | 2 (2) |
| $S_{21}$ | 0 | 1 (2) |
| $S_{22}$ | 0 | $-4$ (5) |
| $S_{23}$ | 0 | 1 (2) |
| $S_{31}$ | 0 | 1 (2) |
| $S_{32}$ | 0 | 5 (2) |
| $S_{33}$ | 0 | $-10$ |
| | | |
| Goodness of fit | 1.16 | 0.96 |
| $wR(U)$ | 0.011 | 0.053 |

### (b) M.s. amplitudes of internal vibrations ($\text{Å}^2 \times 10^{-4}$)

Columns are as follows: $\Delta_{A-B} = \ <\ u_B^2\ > - <\ u_A^2\ >$, which is the difference in m.s. amplitudes of nuclear displacement along the interatom vector for nuclei $A$ and $B$ as determined from $U^{ij}$, (Hirshfeld, 1976). $U^{ij}$ are the components of the difference tensor $U^{ij}_{int} = U^{ij}_{obs} - U^{ij}_{ext}$ referred to the local Cartesian axial system for each H nucleus. The local axes are defined in terms of the internuclear vectors $\mathbf{u}$ and $\mathbf{v}$. For example, for the H1N1 atom of the spermine cation, $\mathbf{u}$ is along the N1—H1N1 bond and $\mathbf{v}$ is along the N1—H2N1 bond. The local $x$ axis is along the N1—H1N1 bond; the local $y$ axis is normal to the N1—H1N1 bond and within the $NH_2$ plane; and the local $z$ axis is along $\mathbf{u} \times \mathbf{v}$ which is normal to the plane of the $NH_2$ group. Thus, $U^{11}$ is an internal m.s. displacement along the N1—H1N1 bond, $U^{22}$ is a displacement in the H2N1—N1—H1N1 plane and $U^{33}$ is a displacement normal to the H2N1—N1—H1N1 plane. For the HO4 H atom the first local $x$ axis is along the O—H bond; the local $y$ axis is in the P—O—H plane normal to the O—H bond and the local $z$ axis is normal to the P—O—H plane. For the second local axial system for the HO4 atom the $x$ axis is along the HO4$\cdots$O2 hydrogen bond, the $y$ axis is normal to the HO4$\cdots$O2 hydrogen bond and within the O2$\cdots$HO4—O4 plane, and the $z$ axis is normal to the O2$\cdots$HO4—O4 plane. $U_1$, $U_2$ and $U_3$ are the principal values of $U^{ij}_{int}$.

## Table 2 (*cont.*)

|  | $\Delta_{A-H}$ | $U^{11}$ | $U^{22}$ | $U^{33}$ | $U^{12}$ | $U^{13}$ | $U^{23}$ | $U_1$ | $U_2$ | $U_3$ |
|---|---|---|---|---|---|---|---|---|---|---|
| H1N1 | 49 (30) | 41 | 95 | 119 | 11 | 7 | $-7$ | 38 | 96 | 121 |
| H2N1 | 67 (19) | 60 | 51 | 112 | $-19$ | 7 | 3 | 75 | 35 | 113 |
| H1N2 | 39 (34) | 25 | 148 | 152 | $-37$ | $-20$ | $-5$ | 12 | 159 | 154 |
| H2N2 | 65 (20) | 67 | 131 | 53 | $-75$ | 26 | 18 | 87 | 135 | 28 |
| H3N2 | 56 (19) | 48 | 127 | 90 | $-29$ | 12 | 78 | 66 | 191 | 8 |
| HO4 | 65 (26) | 57 | 109 | 13 | 9 | 3 | 20 | 56 | 114 | 9 |
| HO4 |  | 56 | 99 | 24 | 1 | 4 | 36 |  |  |  |

† For the cation, the constraint $S_{ij} = 0$ was imposed since the spermine cation lies on a crystallographic inversion center.

For the H1N1 nucleus the principal values are similar to the diagonal components of the $U^{ij}_{int}$ tensor and the off-diagonal components are relatively small. Thus, the principal values are for vibrations in directions close to those of the local axial system. However, for the other ammonium hydrogens (H2N1 and the terminal H1N2, H2N2 and H3N2) this is not the case and the off-diagonal terms of the $U^{ij}_{int}$ tensors are significant. The vibrations of these H nuclei seem to be influenced by the effects of intermolecular N—H$\cdots$O hydrogen bonding.

With the hydrogen nucleus omitted, the monohydrogen phosphate anion was analyzed in terms of a simple rigid-body model (Schomaker & Trueblood, 1968). The $U^{ij}_{obs}$ values were fitted to a rigid-body model by least-squares (He & Craven, 1993), resulting in a good fit with $wR = 0.053$ and $S = 0.96$, where $(m - n) = 10$. The rigid-body contribution to the m.s. displacements of the HO4 atomic nucleus, $U^{ij}_{ext}$, was then calculated using the parameters listed in Table 2. The differences ($U^{ij}_{obs} - U^{ij}_{ext}$, are assumed to represent $U^{ij}_{int}$, the intramolecular m.s. displacements. Table 2 also lists these residuals, which have been transformed to a local atomic axial system with $U^{11}_{int}$ along the OH bond, $U^{22}_{int}$ in the P—O—H plane normal to the O—H bond and $U^{33}_{int}$ normal to the P—O—H plane. For the HO4 atom the principal values are for vibrations in directions close to those of the local axial system, but the value of $U^{33}_{int}$, $13 \times 10^{-4}$ $\text{Å}^2$, is smaller than expected. The nonrigid m.s. displacements of HO4 seem to be influenced by the effects of intermolecular O—H$\cdots$O hydrogen bonding. The HO4 atom is involved in a hydrogen bond with O2 of a neighboring monohydrogen phosphate anion (Table 5). Table 2 lists $U^{ij}_{int}$ for the HO4 atoms transformed into a second local axial system. In this axial system $U^{11}_{int}$ is along the HO4$\cdots$O2 hydrogen bond, $U^{22}_{int}$ is normal the the HO4$\cdots$O2 hydrogen bond and within the O2$\cdots$HO4—O4 plane, and $U^{33}_{int}$ is normal to the O2$\cdots$HO4—O4 plane. In this second system the value of $U^{33}_{int}$ is increased to $24 \times 10^{-4}$ $\text{Å}^2$.

## 3. Discussion

### 3.1. Molecular geometry and crystal packing

The bond lengths and angles of the monohydrogen phosphate ion and water molecules, as well as the bond

lengths and angles of the spermine cation, are listed in Table 3.† Thermal vibrational corrections of bond lengths of the C and N atoms are small and within the e.s.d.'s of the uncorrected values. The average values for the C—C and C—N bond lengths corrected for thermal libration are 1.526 (8) and 1.489 (5) Å. The C—C and C—N bond lengths are all in close agreement. The largest difference of a bond length from the average value is 0.01 Å for C1—C1'. Thermal vibrational corrections for the C—H and N—H bond lengths have not been made, since it is expected that the corrections for harmonic and anharmonic motion are likely to be almost equal and opposite (Ibers 1959; Craven & Swaminathan, 1984), and with an uncertainty comparable to the net correction. The average C—H and N—H bond lengths are 1.098 (4) and 1.054 (8) Å. The length of the P—O4 bond, 1.591 Å, is significantly longer than the other P—O bonds, as is to be expected. The monohydrogen phosphate ion has O—P—O bond angles in the range 104.5 (2)–113.1 (2)° (Table 3) with the smaller angles involving the longer P—O4 bond. The average Ow—H bond length is 0.96 (2) Å.

The spermine tetracation, $[NH_3(CH_2)_3NH_2(CH_2)_4$-$NH_2(CH_2)_3NH_3]^{4+}$, as shown in Fig. 1, has an extended all *trans* conformation. It has a crystallographic inversion center and the non-H atoms of the spermine chain are almost coplanar, with the largest deviation out of the best least-squares plane being 0.11 Å. The torsion angles of the spermine tetracation are listed in Table 4. In the crystal structure of spermine pyrophosphate hexahydrate (Labadi, Sillanpää & Lönnberg, 1992) the spermine cation also adopts an extended conformation with the largest deviation from a planar arrangement at the C4—C3—N1—C2 segment. The torsion angle about C3—N1 is 171.4 (2)°. The spermine tetracation chain is almost fully extended in the crystal structure of spermine tetranitrate (Jaskólski, 1987), with all bonds *trans* except the *gauche* terminal N2—C5—C4—C3 torsion angle of −65.0 (4)°. In contrast, in the crystal structure of spermine tetrahydrochloride (Giglio, Liquori, Puliti & Ripamonti, 1966) the spermine tetracation is bent with *gauche* turns at the C2—N1 bonds with a C1—C2—N1—C3 torsion angle of 66.0° such that the non-H atoms of the chain consist of three approximately planar groups. In all of these crystal structures the spermine tetracation has a crystallographic center of symmetry. However, there seems to be some conformational flexibility. It is also interesting to consider the spermidine phosphate trihydrate crystal structure (Huse & Iitaka, 1969), in which there are two crystallographically independent spermidine trications $[NH_3^+(CH_2)_3NH_2^+(CH_2)_4NH_3^+]$. Both these trications exist

Table 3. *Selected geometric parameters (Å, °)*

Spermine cation

| | | | |
|---|---|---|---|
| N1—C2 | 1.493 (2) | N2—H3N2 | 1.067 (5) |
| N1—C3 | 1.485 (2) | C1—H1C1 | 1.092 (5) |
| N2—C5 | 1.485 (2) | C1—H2C1 | 1.101 (5) |
| C1—C1' | 1.533 (3) | C2—H1C2 | 1.096 (5) |
| C1—C2 | 1.518 (3) | C2—H2C2 | 1.097 (5) |
| C3—C4 | 1.518 (3) | C3—H1C3 | 1.093 (5) |
| C4—C5 | 1.525 (3) | C3—H2C3 | 1.098 (5) |
| N1—H1N1 | 1.051 (5) | C4—H1C4 | 1.099 (5) |
| N1—H2N1 | 1.054 (5) | C4—H2C4 | 1.106 (5) |
| N2—H1N2 | 1.053 (5) | C5—H1C5 | 1.100 (5) |
| N2—H2N2 | 1.047 (5) | C5—H2C5 | 1.096 (5) |

Monohydrogen phosphate

| | | | |
|---|---|---|---|
| P—O1 | 1.521 (3) | P—O4 | 1.591 (3) |
| P—O2 | 1.528 (3) | O4—HO4 | 1.004 (5) |
| P—O3 | 1.532 (3) | | |

Water molecules

| | | | |
|---|---|---|---|
| W1—H2W1 | 0.990 (6) | W2—H2W2 | 0.964 (12) |
| W1—H1W1 | 0.949 (13) | W2—H3W2 | 0.943 (11) |
| W1—H3W1 | 0.925 (11) | W3—H1W3 | 0.981 (5) |
| W2—H1W2 | 0.968 (6) | W3—H2W3 | 0.979 (5) |

Spermine cation

| | | | |
|---|---|---|---|
| C2—N1—C3 | 111.5 (1) | H2N2—N2—H3N2 | 108.7 (4) |
| N2—C5—C4 | 112.4 (2) | H1N1—N1—H2N1 | 108.7 (4) |
| N1—C2—C1 | 112.4 (2) | H1C1—C1—H2C2 | 107.2 (4) |
| N1—C3—C4 | 112.1 (2) | H1C2—C2—H2C2 | 108.9 (4) |
| C1'—C1—C2 | 110.4 (2) | H1C3—C3—H2C3 | 108.1 (4) |
| C3—C4—C5 | 108.8 (2) | H1C4—C4—H2C4 | 108.8 (4) |
| H1N2—N2—H2N2 | 108.5 (4) | H1C5—C5—H2C5 | 108.2 (4) |
| H1N2—N2—H3N2 | 107.9 (4) | | |

Monohydrogen phosphate

| | | | |
|---|---|---|---|
| O1—P—O2 | 113.1 (2) | O2—P—O4 | 107.6 (2) |
| O1—P—O3 | 110.1 (2) | O3—P—O4 | 104.5 (2) |
| O2—P—O3 | 112.4 (4) | HO4—O4—P | 117.4 (3) |
| O1—P—O4 | 108.7 (2) | | |

Water molecules

| | | | |
|---|---|---|---|
| H1W1—W1—H2W1 | 106.8 (8) | H1W2—W2—H3W2 | 112.5 (8) |
| H1W1—W1—H3W1 | 125.9 (10) | H2W2—W2—H3W2 | 114.7 (10) |
| H2W1—W1—H3W1 | 106.8 (8) | H1W3—W3—H2W3 | 105.7 (5) |
| H1W2—W2—H2W2 | 110.5 (8) | | |

Table 4. *Torsion angles (°) of the spermine backbone C and N atoms*

Sign is positive if, viewed from second to third atom, clockwise motion superimposes first on fourth atom.

| | | | |
|---|---|---|---|
| C3—N1—C2—C1 | 174.8 (2) | C1'—C1—C2—N1 | 176.6 (2) |
| C2—N1—C3—C4 | −177.5 (2) | N1—C3—C4—C5 | −178.8 (2) |
| C2—C—C1'—C2' | 180.0 | C3—C4—C5—N2 | −175.2 (2) |

in a normal extended configuration, with one being almost coplanar, while the second is slightly rippled, with the largest deviations out of the best least-squares plane being approximately 0.2 Å.

The crystal structure of SPH is made up of two types of alternating sheets. The first consists of spermine tetracations. Monohydrogen phosphate ions and water molecules link by hydrogen bonding to form the second type of sheet. The two types of sheets stack parallel to the (001) plane and are held together by N—H···O hydrogen bonds.

The structure of the tetracation sheet is shown in Fig. 3. The spermine chains are tilted ∼57° from the *b* axis and adjacent chains related by the *a* glide are oppositely inclined. The shortest chain-to-chain distance.

2.37 Å, is between H1C1 and H1C5' (1 + $x$, $y$, $z$). Both spermine nitrogens in the asymmetric unit are fully protonated and four out of the five protons are involved in hydrogen bonds with monohydrogen phosphate anions. The remaining proton of the secondary nitrogen is hydrogen bonded to a water molecule. Distances and angles of hydrogen bonding between sheets as well as within the sheets are listed in Table 5. As would be expected, the hydrogen-bond distances involving the negatively charged monohydrogen phosphate ion are shorter than the hydrogen bonds involving the neutral water molecules.

A projection of the monohydrogen phosphate–water sheet along the $c$ axis, Fig. 4($a$), shows the hydrogen bonding of the monohydrogen phosphate ions and water molecules within the sheet. This sheet has the composition $HPO_4^{2-}.3H_2O$ and contains parallel chains of monohydrogen phosphate ions running along the $a$ axis which are held together by water molecules. As predicted by Iitaka & Huse (1965), the water molecules form a network of hydrogen bonds which resembles a distorted ice-Ih structure. The repeat distance of these water chains is $a = 7.931$ Å at 125 K. This is analogous to the length of the $c$ axis in ice-Ih, which is 7.32 Å (Rottger, Endriss, Ihringer, Doyle & Kuhs, 1994). The bond distances and angles of the disordered H atoms are compared with those of ice-Ih in Table 6 (Kuhs & Lehmann, 1983). Although the bond lengths between the two structures are comparable, the coordination of the water O atoms of the spermine structure is markedly distorted from the regular tetrahedral angle. The disordered water molecules in this structure have H—O—H bond angles in the range 106.8 (8)–125.9 (10)°. Also, the oxygen atoms ($W$1 and $W$2) each have three oxygen nearest-neighbors rather than four as in ice-Ih. The disordered H-

### Table 5. Hydrogen-bonding geometry (Å, °) in SPH

| Between sheets | | |
|---|---|---|
| N—H···O—P | H2N1···O3 | 1.773 (5) |
| | N1—H2N1···O3 | 165.1 (4) |
| | H1N2···O1 | 1.669 (5) |
| | N2—H1N2···O1 | 172.5 (4) |
| | H2N2···O2 | 1.837 (5) |
| | N2—H2N2···O2 | 173.9 (4) |
| | H3N2···O1 | 1.620 (5) |
| | N2—H3N2···O1 | 175.5 (4) |
| N—H···O$_W$ | H1N1···W3 | 1.856 (5) |
| | N1—H1N1···W3 | 165.9 (4) |
| **Within water/phosphate sheet** | | |
| O$_W$H···OW | H1W1···W2 | 1.810 (12) |
| | W1—H1W1···W2 | 175.6 (11) |
| | H3W1···W1' | 1.836 (11) |
| | W1—H3W1···W1' | 177.2 (10) |
| | H1W2···W3 | 1.875 (6) |
| | W2-H1W2···W3 | 172.9 (5) |
| | H2W2···W1 | 1.803 (12) |
| | W2—H2W2···W1 | 170.2 (10) |
| | H3W2···W2' | 1.819 (11) |
| | W2—H2W2···W2' | 171.2 (10) |
| O$_W$H···O—P | H2W1···O3 | 1.731 (5) |
| | W1—H2W1···O3 | 176.2 (5) |
| | H1W3···O3 | 1.736 (5) |
| | W3—H1W3···O3 | 175.0 (5) |
| | H2W3···O2 | 1.845 (5) |
| | W3—H2W3···O2 | 175.1 (5) |
| | HO4···O2 | 1.650 (5) |
| | O4—HO4···O2 | 166.8 (4) |

atom positions are shown more clearly in Fig. 4($b$). The two water molecules each have one ordered hydrogen position and two disordered hydrogen positions, each with an occupancy of 0.5. Placement of one H atom into one of the two possible disordered positions will consequently determine the configuration of the entire chain. We propose a random arrangement of the two chain configurations.

### 3.2. Spermine–DNA interactions

In solution spermine forms a complex with the anionic phosphate backbone of DNA such that there is a constant ratio of negative charge from phosphate groups and positive charge from the spermine tetracation regardless of the base composition of DNA (Hirschman, Leng & Felsenfeld, 1967; Braunlin, Strick & Record, 1982). The SPH structure provides a relevant model for phosphate/spermine interactions involving native DNA. As previously described by Iitaka & Huse (1965), the arrangement of phosphate groups in this structure resembles that found in B-DNA. The separation of monohydrogen phosphate chains between sheets along the $c$-translation period of 6.856 (2) Å is similar to the distance between successive phosphate groups along the B-DNA chain of approximately 6.7 Å. Also, the perpendicular distance between two monohydrogen phosphate chains of $b/2$ or 11.579 (5) Å may be compared with the average perpendicular distance of phosphates across the minor groove of B-DNA, 11.5 Å. The spermine tetracation forms hydrogen bonds to the phosphates, holding monohydrogen phosphate chains
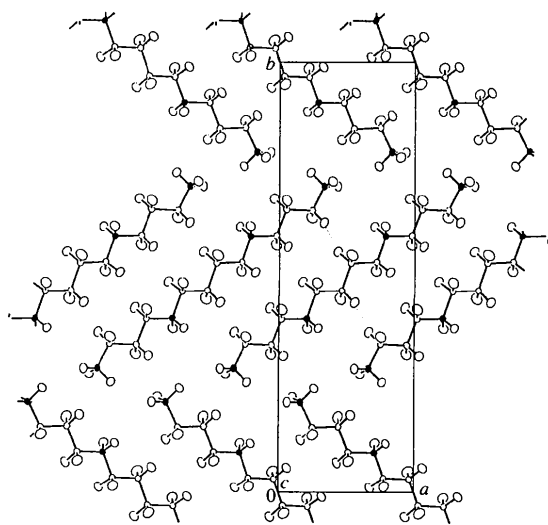


Fig. 3. The cation molecular sheet. N atoms are solid. Dotted lines show the closest chain-to-chain distance, 2.37 Å.

Table 6. *Comparison of the molecular geometry of the neutron structure of ice-Ih with the SPH structure's water molecules, W1 and W2 with two disordered hydrogens each (H1W1 and H3W1, and H2W2 and H3W2)*

| Ice-Ih (Kuhs & Lehmann, 1983) at 123 K | | | |
|---|---|---|---|
| O—O' | 2.751 | O—H2 | 1.004 |
| O—O'' | 2.753 | H1—H1' | 0.735 |
| O—H1 | 1.008 | H2—H2' | 0.754 |

| SPH at 125 K | | | |
|---|---|---|---|
| W1—W1' | 2.759 (4) | W2—H2W2 | 0.96 (1) |
| W2—W2' | 2.754 (4) | W2—H3W2 | 0.94 (1) |
| W1—W2 | 2.758 (4) | H1W1—H2W2 | 0.86 (2) |
| W1—H1W1 | 0.95 (1) | H3W1—H3W1' | 0.91 (2) |
| W1—H3W1 | 0.93 (1) | H3W2—H3W2' | 0.90 (2) |

| Ice-Ih (Kuhs & Lehmann, 1983) at 123 K | | | |
|---|---|---|---|
| O'—O—O'' | 109.34 | H1—O—H2 | 109.40 |
| O''—O—O'' | 109.60 | H2—O—H2 | 109.54 |

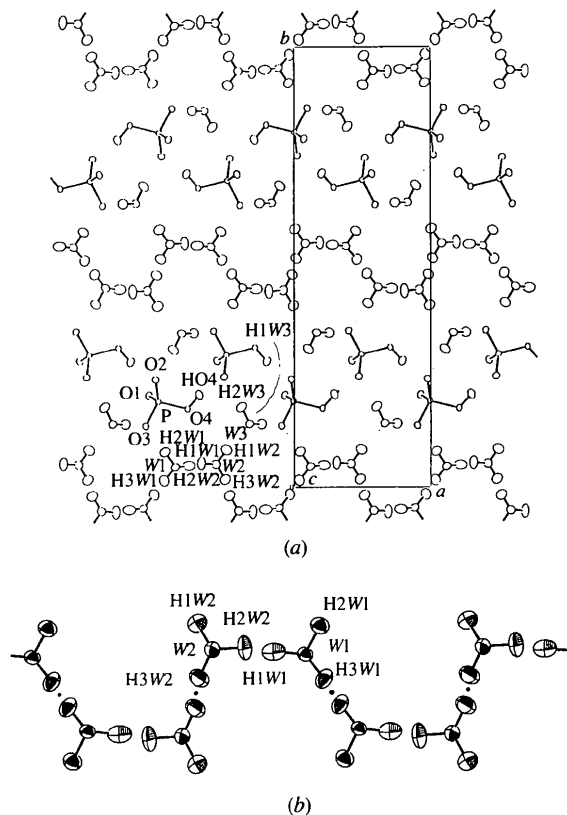| SPH at 125 K | | | |
|---|---|---|---|
| W2—W1—W1' | 123.8 (1) | H1W1—W1—H2W1 | 106.8 (8) |
| W1—W2—W2' | 103.1 (1) | H2W1—W1—H3W1 | 106.8 (8) |
| H1W1—W1—H3W1 | 125.9 (10) | H1W2—W2—H2W2 | 110.5 (8) |
| H2W2—W2—H3W2 | 114.7 (10) | H1W2—W2—H3W2 | 112.5 (8) |



(a)



(b)

Fig. 4. (a) The monohydrogen phosphate–water sheet. The protons H1W1, H3W1, H2W2 and H3W2 are disordered, each occupying two sites with equal probability. Hydrogen bonds are shown as dotted lines. (b) Thermal ellipsoid plot for the ice-like chain of water molecules at 50% probability for enclosing the atomic nuclei (Johnson, 1976). Black dots represent inversion centers. The protons H1W1, H3W1, H2W2 and H3W2 are disordered, each occupying two sites with equal probability.

within each sheet together as well as holding together monohydrogen phosphate chains in adjoining sheets. The SPH structure presently studied provides a good model for either the binding of spermine along the phosphate backbone of DNA or across the minor groove of DNA.

## References

Blessing, R. H. (1989). *J. Appl. Cryst.* **22**, 396–397.

Braunlin, W. H., Strick, T. J. & Record, M. T. Jr (1982). *Biopolymers*, **21**, 1301–1314.

Craven, B. M. & Swaminathan, S. (1984). *Trans. Am. Crystallogr. Assoc.* **20**, 133–135.

Craven, B. M. & Weber, H. P. (1987). *NOOT. Computer Program for Least-Squares Refinement with Neutron Diffraction Data*. Technical Report. Department of Crystallography, University of Pittsburgh, Pittsburgh, PA 15260, USA.

Gao, Q., Weber, H. P., Craven, B. M. & McMullan, R. K. (1994). *Acta Cryst.* B**50**, 695–703.

Giglio, E., Liquori, A. M., Puliti, R. & Ripamonti, A. (1966). *Acta Cryst.* **20**, 652–656.

He, X. & Craven, B. M. (1993). *Acta Cryst.* A**49**, 10–22.

Hirschman, S. Z., Leng, M. & Felsenfeld, G. (1967). *Biopolymers*, **5**, 227–233.

Hirshfeld, F. L. (1976). *Acta Cryst.* A**32**, 239–244.

Huse, Y. & Iitaka, Y. (1969). *Acta Cryst.* B**25**, 498–509.

Ibers, J. A. (1959). *Acta Cryst.* **12**, 251–252.

Iitaka, Y. & Huse, Y. (1965). *Acta Cryst.* **18**, 110–121.

Jaskólski, M. (1987). *Acta Cryst.* C**43**, 1375–1378.

Johnson, C. K. (1970). *Thermal Neutron Diffracton*, edited by B. T. M. Willis, pp. 132–160. Fairlawn, New Jersey: Oxford University Press.

Johnson, C. K. (1976). *ORTEPII*. Report ORNL-5138. Oak Ridge National Laboratory, Tennessee, USA.

Koester, L. (1977). *Neutron Physics*, edited by G. Höhler, p. 1. Berlin: Springer

Kuhs, W. F. & Lehmann, M. S. (1983). *J. Phys. Chem.* **87**, 4312–4313.

Labadi, I., Sillanpää, R. & Lönnberg, H. (1992). *J. Chem. Soc. Dalton Trans.* pp. 765–767.

Leeuwenhoek, A. van (1678). *Philos. Trans. R. Soc. London*, **12**, 1040.

Liquori, A. M., Constantino, L., Crescenti, V., Elia, V., Giglio, E., Puliti, R., Savino, M. de S. & Vitagliano, V. (1967). *J. Mol. Biol.* **24**, 113–122.

Luo, J., Ruble, J. R., Craven, B. M. & McMullan, R. K. (1996). *Acta Cryst.* B**52**, 357–368.

McMullan, R. K. (1976). *DIFSYN Differential Fourier Synthesis Program*. Unpublished work.

Morris, D. R. & Marton, L. J. (1981). *Polyamines in Biology and Medicine*. New York: Marcel Dekker.

Rottger, K., Endriss, A., Ihringer, J., Doyle, S. & Kuhs, W. F. (1994). *Acta Cryst.* B50, 644–648.

Sabine, T. M. (1992*a*). *International Tables for Crystallography*, Vol. C, pp. 530–533. Dordrecht: Kluwer Academic Publishers.

Sabine, T. M. (1992*b*). *Modifications to Treat Extinction in the Computer Program NOOT for Least-Squares Refinement with Neutron Diffraction Data.* Unpublished work.

Schomaker, V. & Trueblood, K. N. (1968). *Acta Cryst.* B24, 63–76.

Shiono, R. (1972). *FOUR. Three-Dimensional Fourier Synthesis Program.* Technical Report. Department of Crystallography, University of Pittsburgh, Pittsburgh, PA 15260, USA.

Spackman, M. A. (1987). Unpublished work.

Tabor, C. W. & Tabor, H. (1976). *Annu. Rev. Biochem.* 45, 285–306.

Templeton, L. K. & Templeton, D. H. (1973). *Am. Crystallogr. Asssoc. Meeting.* Abstracts, p. 143. Storrs, Connecticut.

Tsuboi, M. (1964). *Bull. Chem. Soc. Jpn*, 37, 1515.